Study of the durability of ferritic - austenitic steel samples after cyclical fatigue impact

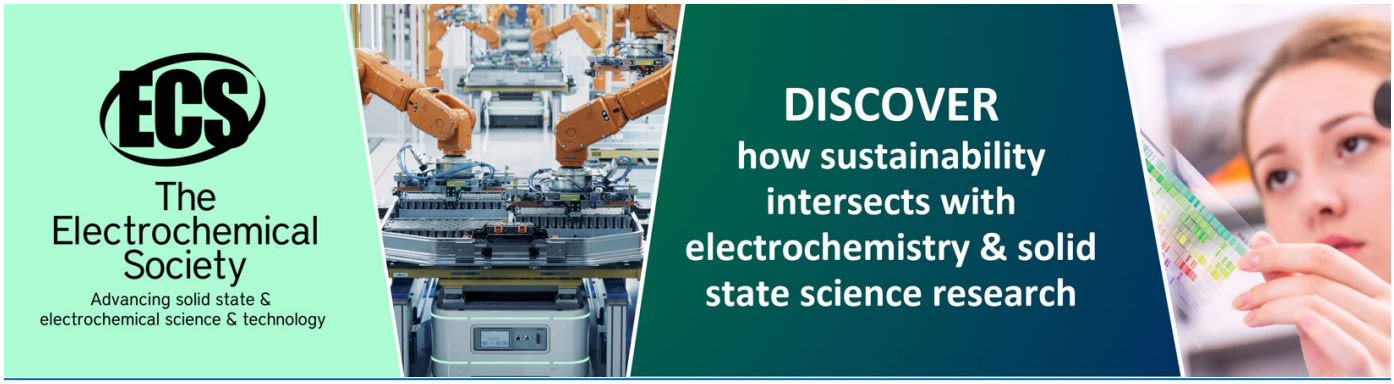

Study of the durability of ferritic - austenitic steel samples after cyclical fatigue impact

Georgi Georgiev[1], Yaroslav Argirov[1], Tatyana Mechkarova[1], Daniela Spasova[1], Aneliya Stoyanova [1]

[1]Technical University of Varna, Material Science and Technology Department, Studentska Street 1, Varna, Bulgaria

[*]Corresponding author's e-mail: t.mechkarova@tu-varna.bg

Abstract. The purpose of this article is to investigate the fatigue strength of corrosion resistant ferritic austenitic steels used in marine equipment. Two groups of sheet steel samples were prepared: the first group were reference parts and the second group of samples were welded. The fatigue tests were performed with specially developed vibrating equipment. The destroyed surfaces were examined by optical microscopy, and the phase composition by X-ray diffraction analysis. Fatigue strength was evaluated by the number of cycles needed for a crack at a certain alternating load. Fatigue tests show how multi-cyclical fatigue affects the formation and development of a fatigue crack, and metallographic and X-ray diffraction analysis shows the phase changes occurring in the structure of SAF 2507 steel.

1. Introduction

Very often in practice, especially in drilling in marine conditions, the use of corrosion-resistant steels is required. They are deployed at great depths and are subjected to cyclical loading [2,3,4] due to the dynamic sea processes and their connection with the drilling ship. Ferritic - austenitic steels, such as duplex steel SAF 2507 (1.4410) are very sensitive to minimal changes in the chemical composition of the technological process of their production, as well as to the modes selected for their welding and cooling, affecting their service life [5,6,7,8,9]. In this example, the causes of cracks in SAF 2507 duplex steel parts, which form drilling equipment subjected to fatigue impact, are analyzed (Fig. 1).

a b

Figure 1. Machine parts of duplex steel operating in sea conditions at a depth of 70m: a) pipeline with welding; b) flange connection

2. Experimental study

2.1. Methodology for obtaining of samples

For the purposes of this study, steel SAF2507 (ASTM S32750) with the following chemical composition was used (Table 1).

Table 1. Chemical composition of steel SAF2507 [1]

C	Si	Mn	P	S	Cr	Ni	Mo
≤0.030	≤0.8	≤1.2	≤0.025	≤0.015	25	7	4

In order to reduce the temperature effect influencing the structural changes, a laser is used to cut the test samples. Fig. 2 shows laser-cut unwelded and welded samples.

a b

Figure 2. Laser cut samples
a) unwelded; b) welded

The unwelded samples (fig. 2-a) are laser cut from a plate with dimensions 350mm by 200mm and thickness 3mm. Welded samples (fig.2-b) are made of two plates measuring 150mm by 350mm with a thickness of 3mm. The two plates are welded unilaterally to each other by manual Shielded Metal Arc Welding (SMAW). ESAB OK 68.82 electrodes were used. The plates are pressed at the four corners to avoid distortion. They are roughly ground so that they can be laser cut. The welded plate is rapidly cooled with water.

2.2. Methodology for determining the geometric dimensions of the test samples and selection of the cyclical loading mode

The determination of the sample frequency and the approximate number of cycles is performed with the software product "SolidWorks" and more precisely with the "frequency" and "fatigue" tool, through which it is possible to select the approximate operating modes of the cyclical load installation.
In order to determine the geometric dimensions of the test samples, the frequency at which the experimental installation will operate is selected. The most stable operation, without fluctuations, is achieved then the installation performs at a frequency of 50 - 80 Hz (determined experimentally). The geometric dimensions are chosen so that the resonant frequency of the samples is in the range of 50 - 60 Hz. With the parameters thus set, the dimensions should be as follows: sample length 172.5 mm, width in the gripping section in the vibrating table 13 mm, width of the loose section 10 mm.
Figure 3 shows all other geometric dimensions of the tested samples.

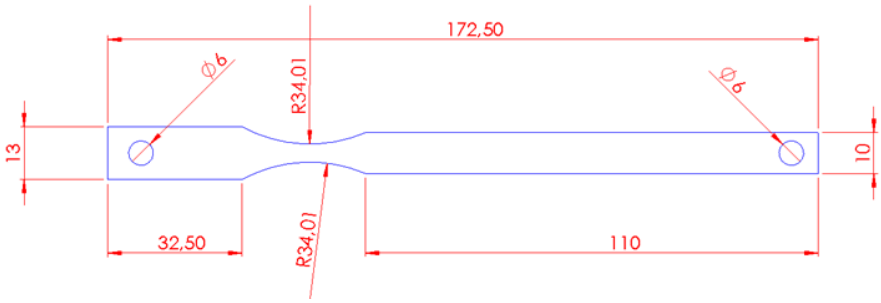

Figure 3. Dimensions of the test samples

Using the "sketch" and "features" tools of SolidWorks, a 3D model of the sample is created and its material is selected.

The first step of the simulation analysis is to select "New study" from the "Study Advisor" menu. Of the types of analyses, "frequency" is the one chose on this occasion, which searches the natural frequencies, as well as visually showing their shape and displacement in case of vibrations from the resulting resonance (fig. 4).

Figure 4. Determination of natural frequency in a 3D model of the test sample

The study obtained a result of 55.9Hz, and with the increase of the 3D model length, the operating frequency decreases.

The second step in the methodology is the study of the test sample for the maximum stresses and displacements that will be created. It is necessary to determine the displacement of the vibrating table at a maximum operating mode of 80N by means of "linear dynamic - harmonic". The results of the analysis show that the stresses in the gripping zone occur in the range of 800 MPa to 830 MPa, which exceeds the stiffness of the material many times and its destruction in this range is inevitable.

To determine the approximate number of cycles, we use the "fatigue" menu with the "constant amplitude" submenu, which is added to the "loading" tool, which is part of the fatigue study. After performing the simulation analysis, the required number of cycles for failure in the range of maximum stresses was established at 32000, and at the same time it was found that the destruction process will last about 10 minutes at an operating frequency of 55 Hz.

2.3. Fatigue test installation

The samples are firmly fixed in a special device made for the specific vibrating table. Accelerometers are used to measure acceleration. The software (National Instruments) enables determination of the moment of the crack formation, which in most cases is visible only at high magnification (fig.5).

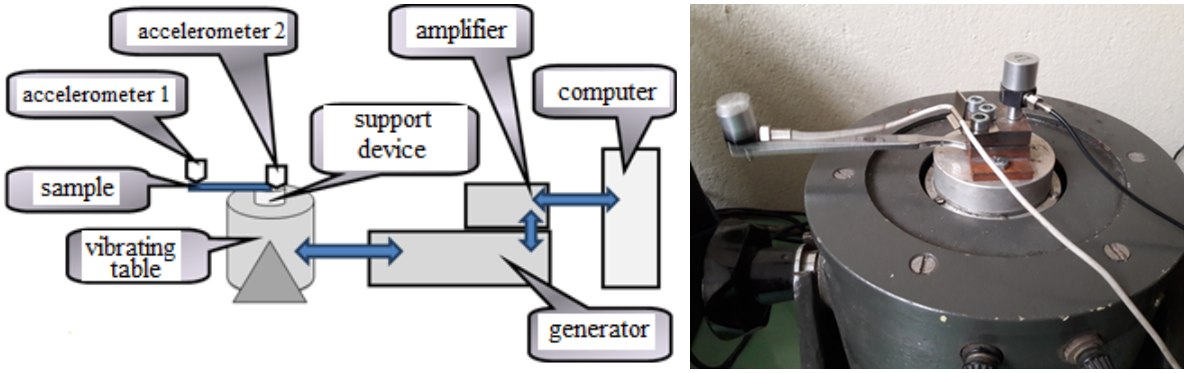

Figure 5. Diagram of the installation for determining the fatigue strength of the material

3. Results of the experimental study

3.1. Fatigue test results

The results of the cyclical tests of the samples that have not been welded are shown in Table 2. The limit observed below which no cracks form is 480 MPa (in the range up to $1x10^7$ cycles). Based on the data obtained (Table 2) the fatigue curve is drawn in fig. 6.

The samples with positions 13, 14, 15, 16, 17and 18 in table 2 were not destroyed within the study range, they are shown by an arrow in fig.6-a. The sample position 11 show values that do not fall within the normal deviation of 5%.

The results of the study of the fatigue strength of the welded samples in the area of the weld metal are shown in table 3. The cyclical tests were performed in the range from 280 MPa to 470 MPa. The fatigue limit in the range from 10^4 to 10^7 cycles was studied. The limit observed below which no cracks from is 340 MPa (in the range up to $1x10^7$ cycles). Based on the data obtained (table 3), the fatigue curve fig. 6-b was compiled. The sample position 30 in table 3 were not destroyed within the studied range, they are shown by an arrow in fig.6-b.

Table 2 The experimental results of the cyclical tests of the samples that have not been welded

Sample №	1	2	3	4	5	6	7	8	9
Load (MPa)	715	640	572	562	560	557	555	550	520
Cycle ($1x10^6$)	0.11	0.25	0.2	0.25	0.32	0.3	0.3	0.33	1

Table 2- continued

Sample №	10	11	12	13	14	15	16	17	18
Load (MPa)	495	370	485	480	470	390	320	290	240
Cycle ($1x10^6$)	0.5	1.3	2	10	10	10	10	10	10

Table 3 The experimental results of the cyclical tests of the welded samples

Sample №	21	22	23	24	25	26	27	28	29	30
Load (MPa)	470	425	415	405	395	385	380	375	360	340
Cycle ($1x10^6$)	0.07	0.21	0.5	0.92	0.94	1.2	2.1	3.3	5.56	10

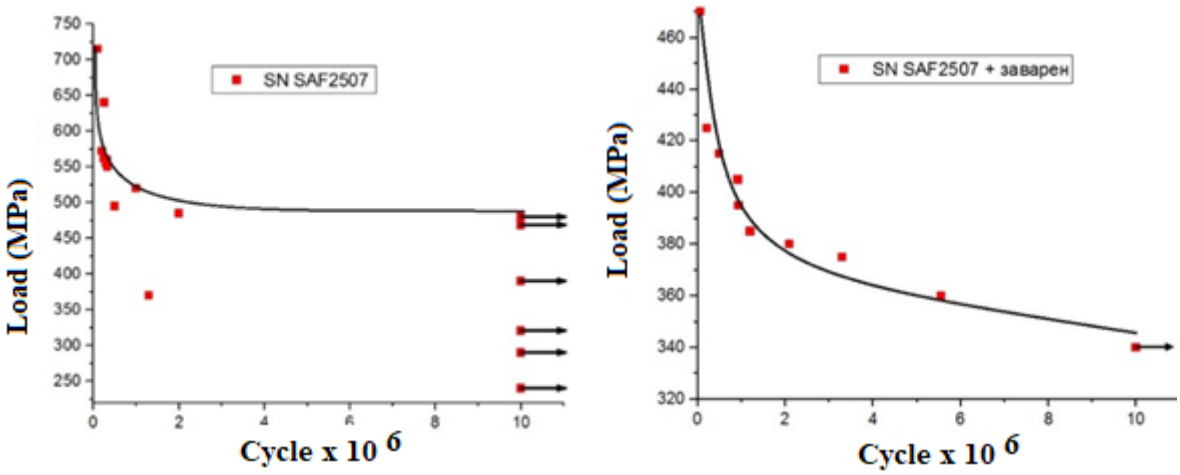

а) б)

Figure 6. S-N curve of SAMF2507 steel samples: a) unwelded; b) welded

3.2. Results of metallographic tests

Before the samples are placed in fatigue conditions, they must be perfectly sanded, going from sandpaper 100 to 1000. This is followed by polishing to a perfectly smooth surface and the absence of any scratches. When the samples are destroyed, only the fracture of the respective sample is visible, but it does not give a clear idea and assessment of the parameters and features of the crack. Using a specially made device (fig. 7) the parts of the already destroyed sample are pressed against each other along the crack. It was decided to place two samples simultaneously in order to polish them evenly.

This is followed by grouting with polyester resin, which helps to clearly delineate the edges and prevents the incorrect reflection of light in the subsequent microstructural analysis. Using a solution of HCl, HNO_3 and NaCl (MACC60) followed by subsequent polishing and drying, we corrode the structure around the crack. The process is repeated until the set result is achieved, and in this case it is a clear delineation of the grain boundaries. Through the developed methodology we get clear images of the sliding lines, and the reason for the crack to stop or deviate. The examination of the microstructure is performed by a metallographic microscope.

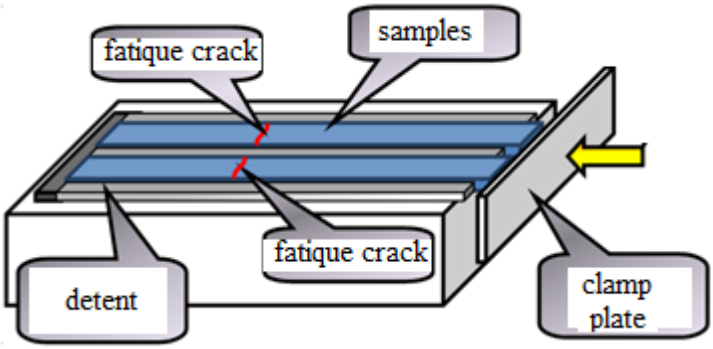

Figure 7. Schematic of a device for microstructural analysis of cracks

Figure 8 shows the crack that passed through the weld metal on the forward facing surface. The crack is offset from the perpendicular side section by a small angle. In addition, a zigzag pattern is observed, which is due to the dendritic structure in the weld metal, in contrast to the crack in the base metal, which has a linear character.

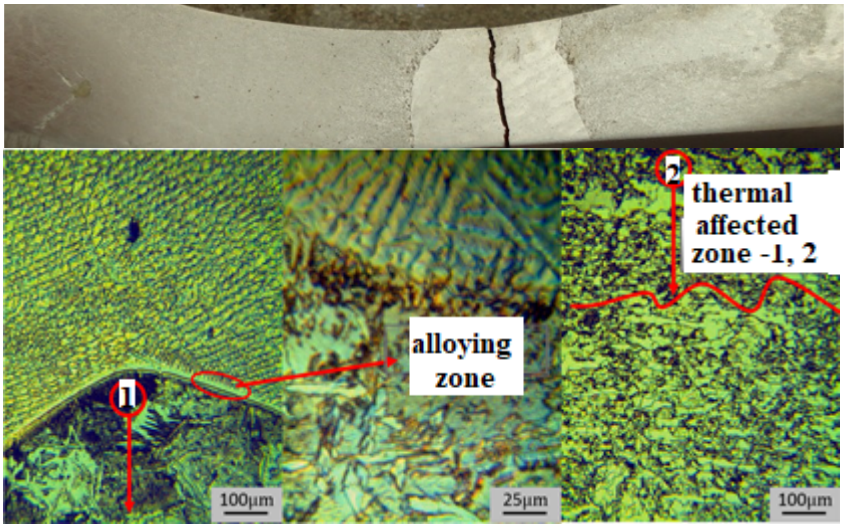

a b c

Figure 8. Microstructure of a welded sample, a) alloying zone, X100; b) alloying zone, X400; c) thermal affected zone X100.

Fig. 9 shows the microstructure of the weld metal in the side section. The development of the crack in the lateral section passes through the weld metal of the dendrite crossing the transcrystalline dendritic grains. The structures on fig. 9-a show the beginning of a crack development, fig. 9-b the lower end of the crack, and fig. 9-c shows the pattern through the middle part of the sample.

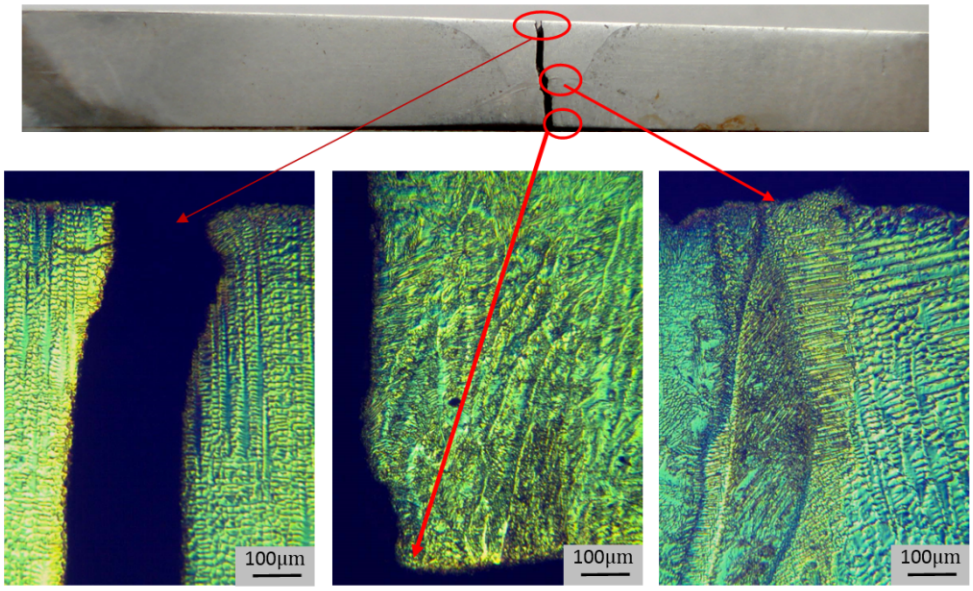

a b c

Figure 9. Microstructure of a sample in side section: a) focus of the crack X100; b) area near the crack in the welded metal X100; c) the area between the two welds X100

3.3. *X - ray diffraction analysis of ferritic - austenitic steel samples*

The studies were performed using an X-ray diffractometer URS-50IM, in the emission of a chromium anode, using a vanadium filter. The integral area of the two phases is determined using the Graph software [10].

- *in delivery condition of SAF 2507 steel*

Fig. 10 shows the radiograph of the unwelded samples in the area of the base material. The quantitative ratio between the two phases was established by the research conducted as γ - Fe (111) = 34%, and α - Fe (110) = 66%. The X-ray structural analysis performed shows the presence of γ - Fe (111) and α - Fe (110), characteristic of ferritic austenitic steels.

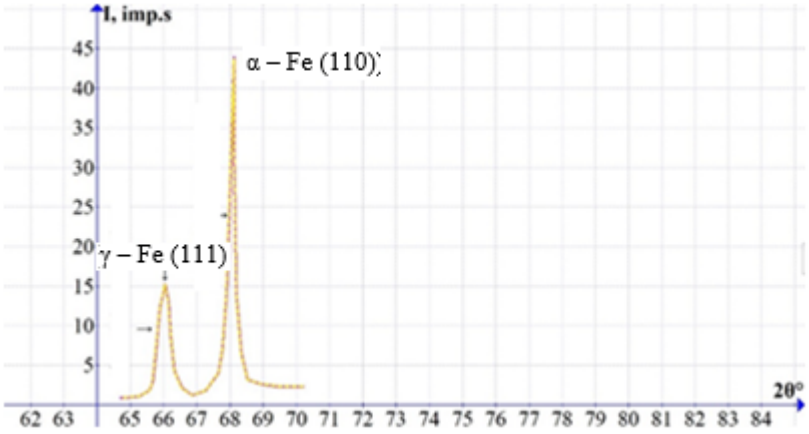

Figure 10. Radiograph of unwelded samples in the area where there is no destruction

Fig. 11 shows a radiograph of the examined samples in the fracture area. The phases and their ratio are determined in this area as γ - Fe (111) = 46%, and α - Fe (110) = 54%. The measured integral areas in the fracture area, respectively, are for γ - Fe (111) = 10.7 deg * imp / sec, and the same phase of the initial sample from Fig.12 has an integral area γ - Fe (111) = 8.5 deg * imp / sec. The broadening of the line observed in the fracture area relative to the initial sample is due to the increased dislocation density and the increased internal stresses (which deform the crystallographic planes).

The case is similar to the ferrite phase, with plane 110 considered. The integral area in the initial state is 13.7 deg * imp / sec, and in the destruction area it is 18.7 deg * imp / sec. Therefore, even in this phase (α - Fe (110)) there is a significant strengthening due to the past deformation processes, during the creation and development of the crack.

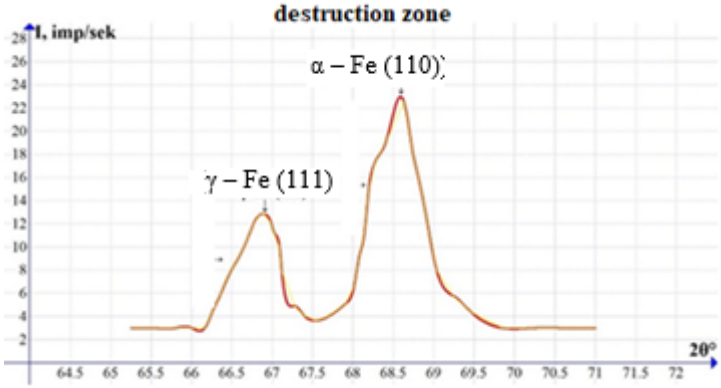

Figure 11. Radiograph in the zone of destruction

- *in the zone of welded metal*

The purpose of the conducted phased qualitative analysis is to establish whether the presence of ferritic - austenitic structure will be preserved at the conducted cooling rate after welding. After the study, the presence of both phases γ - Fe (111) and α - Fe (110) was established (Fig. 12). It was found that the ratio between ferrite and austenite was preserved, as γ - Fe (111) = 60% in the area of the weld metal, and α - Fe (110) = 40%.

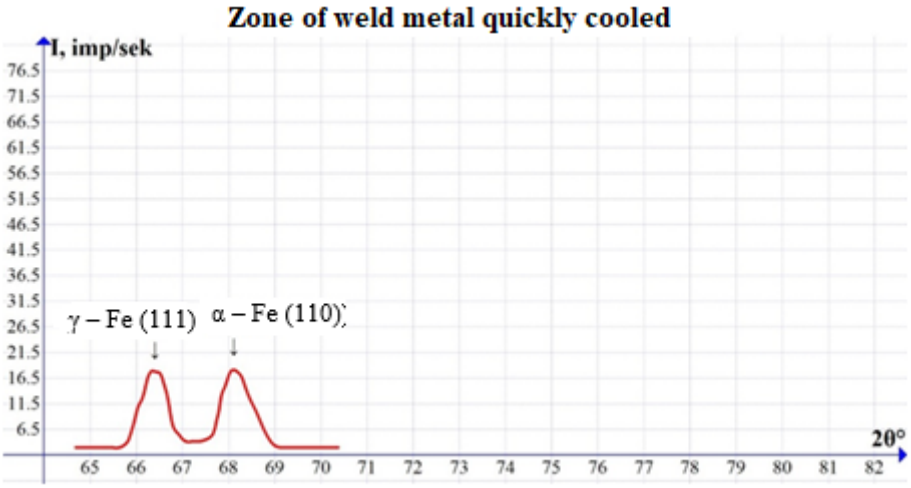

Figure 12. X-ray diffraction analysis in weld metal (γ – Fe (111) и α – Fe (110))

4. Conclusion

1. An increase in the dislocation density and surface internal stresses of γ-Fe (111) and α-Fe (110) was found from the widening of the X-ray line in the fracture area of the unwelded samples.
2. In the weld metal, the X-ray line is identical to that of the unwelded samples while maintaining the ratio between ferrite and austenite as γ - Fe (111) = 60% and α - Fe (110) = 40%.
3. The microstructural analysis found that the crack has a zigzag character in the weld metal, and it is rectilinear in the base material, and in both cases its character is transcrystalline.

References

[1] Sandvik SAF 2507 (http://www.matweb.com/)
[2] Konovalov S, Atroshkina A, Ivanov Y and Gromov V 2010 Evolution of dislocation substructures in fatigue loaded and failed stainless steel with the intermediate electropulsing treatment *MSE A* **12** 3040-3043.
[3] Johannson J and Oden M 2000 Load sharing between austenite and ferrite in a duplex stainless steel during cyclic loading *Met Mater Trans* **A31** 1557
[4] Goh Ch and Yip T 2002 Lowcycle fatigue behavior on duplex stainless steels *Mat. Trans.* **A33** 3433
[5] Duber O, Kunkler B, Krupp U, Christ H and Fritzen C 2006 Experimental characterization and two-dimensional simulation of short crack propagation in an austenitic-feritic suplex steel *Intl J Fatigue* **28** 983
[6] Chai G 2006 Microstructural aspects of duplex steel during high cycle and very high cycle fatigue *Intl J Fatigue* **28** 1533
[7] Callister W 2007 *Materials Science and Engineering: An Introduction* JW& SI USA p15
[8] Alvarez A 2010 Lowcycle fatigue behavior on duplex stainless steels *TIIM* **63** 159-65
[9] Левина А, Мальцева А, Архангельская А, Мальцева Т and Озерец Н 2014 *Разработка аустенитно-ферритной стали нового поколения для упругих элементов в точном машиностроении* Екатеринбург pp 12- 15
[10] Миркин Л 1961 *Справочник по рентгеноструктурному анализу поликристаллов* Физматгиз p 39